

# Polariton condensation and lasing in optical microcavities - the decoherence driven crossover

M. H. Szymanska, P. B. Littlewood, and B. D. Simons

*Theory of Condensed Matter, Cavendish Laboratory, Cambridge CB3 0HE, UK*

(July 28, 2018)

We explore the behaviour of a system which consists of a photon mode dipole coupled to a medium of two-level oscillators in a microcavity in the presence of decoherence. We consider two types of decoherence processes which are analogous to magnetic and non-magnetic impurities in superconductors. We study different phases of this system as the decoherence strength and the excitation density is changed. For a low decoherence we obtain a polariton condensate with comparable excitonic and photonic parts at low densities and a BCS-like state with bigger photon component due to the fermionic phase space filling effect at high densities. In both cases there is a large gap in the density of states. As the decoherence is increased the gap is broadened and suppressed, resulting in a gapless condensate and finally a suppression of the coherence in a low density regime and a laser at high density limit. A crossover between these regimes is studied in a self-consistent way analogous to the Abrikosov and Gor'kov theory of gapless superconductivity [1].

42.50.Fx, 03.75.Gg, 42.50.Gy, 42.55.Ah

## I. INTRODUCTION

The miniaturisation and improvement in the quality of optical cavities in recent years led to the achievement of strong-coupling regime of light-matter interaction in many physical systems. The strong coupling regime is characterised by well-developed coupled modes of light and electronic excitations, called polaritons. Polariton splitting has been experimentally observed for atoms [2], quantum wells [3] and bulk excitons [4], excitons in organic semiconductors [5,6], exciton complexes [7] and glass spheres. The strong coupling regime has also been achieved for coupled Josephson junctions [8] in a microwave cavity.

With well-developed modes, that are sharp and have long lifetimes, a natural question becomes the existence of coherent, condensed states. A theoretically constructed polariton condensate is a mixture of coherent state of light and coherent state of massive particles in the media. It is characterised by two order parameters: the coherent polarisation and the coherent photon field and exhibit a gap in the excitation spectrum [9]. Since the polariton condensate would be a source of coherent light the natural question arises how it is different from and how it can be connected to the traditional laser.

The laser is a weak-coupling phenomenon: a coherent state of photons created by stimulated emission from an inverted electronic population due to strong pumping. The polarisation of the medium is heavily damped and the atomic coherence is practically zero. A coherent photon field, oscillating at the bare cavity mode frequency, is the only order parameter in the system [10].

The crossover between a polariton condensate and a laser is sometimes mistakenly attributed to an increase in density and a crossover from bosonic (exciton) degrees of freedom to fermionic particle-hole pairs. The absence

of polariton splitting is associated with disappearance of coherence, which is why experiments are concentrated at low densities. In this work we show that the trend is an opposite one - the condensate is more robust at high densities. One needs to remember that polaritons, and so polariton splitting, are normal state excitation and so disappearance of polariton splitting in the normal state does not indicate what would happen if the system was condensed.

The issue of electronic coherence in polariton condensate is independent of whether the excitations are more “excitonic” or more like a two-component plasma (ionised electron-hole pairs), or indeed whether or not there is saturation (phase-space filling) of the electronic states. It has been shown [9] that although the increase in the density of electronic excitation leads to nonlinearities in the polariton system which cause the collapse of the splitting between the two polariton peaks in the normal state it does not destroy condensation even at very high excitation densities. The saturation in the fermionic space forces the condensate to become more photon like as the excitation density is increased and to have more BCS-like character, but nevertheless the coherence in the media and the gap in the excitation spectrum are present. The change in the density of the electronic excitations leads to the crossover between the regime of BEC of polaritons and collective BCS-like state

This article will argue that the real enemy of condensation is decoherence, not density, and that it is precisely decoherence which drives the polariton condensate towards the laser regime. We show that only the self-consistent inclusion of decoherence processes allows to establish a crossover between an isolated condensate and a laser. The widely used quantum Maxwell-Bloch (Langevin) equations with constant decay rate for polarisation are not correct in a regime when the coherent polarisation is large and the gap in the density of states is

present. We develop a self-consistent method analogous to the Abrikosov and Gor'kov theory of gapless superconductors, which allows us to study the stability of the polariton condensate at low decoherence strength and to established the crossover to laser behaviour as the decoherence is increased.

## II. MODEL

The model we consider in this work is schematically shown in Figure 1. It consists of a set of  $N$  two-level oscill-

lators dipole coupled to a single mode of electromagnetic field confined in a cavity. This system is then subject to various decoherence, pumping and damping processes. These processes can be of a different physical nature, depending on the material, but their exact details are not that important for a general theory. They can be described, similarly to laser theory, as baths of harmonic oscillators coupled to the system in a way that gives the same effect as the real physical environment.

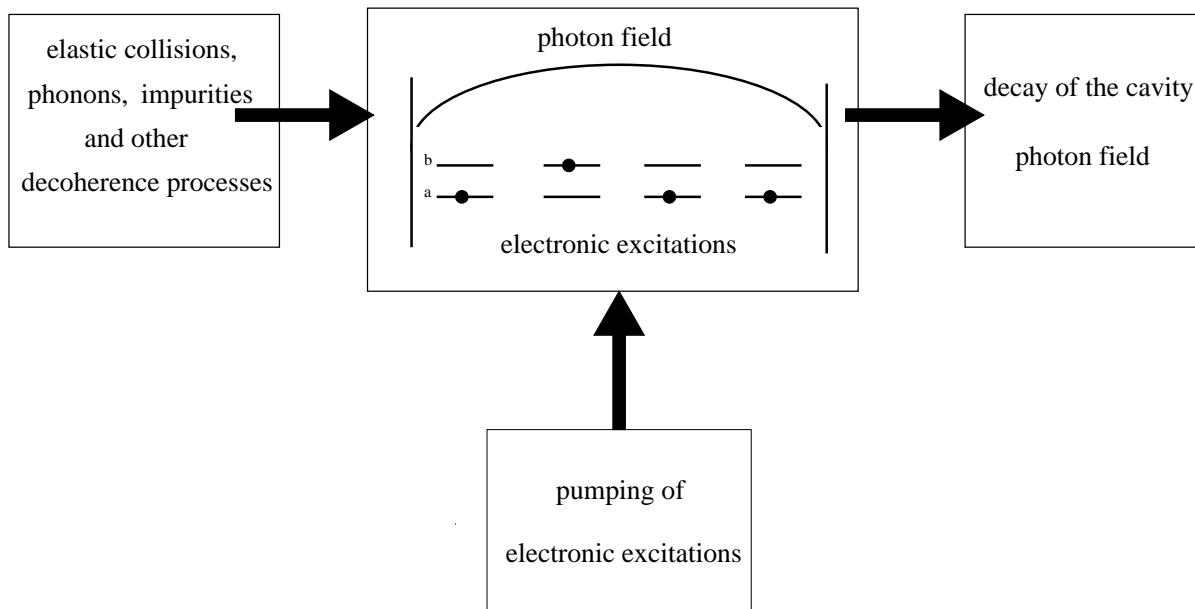


FIG. 1. Sketch of the model studied in this work: the system of two-level oscillators dipole coupled to a single cavity mode interacting with various types of environment.

Our model takes into account the major Coulomb interaction between the electron and hole within the exciton, the phase-space filling effect, disorder in the material (inhomogeneous broadening of excitonic energies) and various types of decoherence effects. However, it does not include screening and Coulomb interactions between excitons. Therefore, it gives a very good description of tightly bound, Frenkel - type of excitons localised by disorder or bound on impurities, molecular excitons in organic materials, atoms in the solid state or Josephson junctions arrays in microwave microcavity. And it gives only a qualitative description within a mean-field approximation for other types of excitons like Wannier excitons or excitons propagating in a sample (see Section VIII).

The model we use is the minimal required to describe

the essential physics. At this stage we do not intend to model any particular medium with its complex interactions which would only make the general picture less clear. More specific details of the particular medium could, however, be included straightforwardly into the formalism. We will discuss this possibility in the Section VIII.

In the following, we consider a system comprised of an ensemble of  $N$  two-level oscillators with an energy  $\epsilon_j$  dipole coupled to a single cavity mode. The corresponding microscopic Hamiltonian takes the form

$$\hat{H}_S = \omega_c \psi^\dagger \psi + \sum_{j=1}^N \epsilon_j (b_j^\dagger b_j - a_j^\dagger a_j) + \sum_{j=1}^N \frac{g_j}{\sqrt{N}} (b_j^\dagger a_j \psi + \psi^\dagger a_j^\dagger b_j) \quad (1)$$

where Fermionic operators  $b_j$  and  $a_j$  annihilate electrons in the upper and lower states respectively, while the Bosonic operator  $\psi$  annihilates the photon. Here the sum extends over the possible sites  $j$  where an exciton can be present (e.g. different molecules or localised states associated with a disorder potential). Matrix elements  $g_j/\sqrt{N}$  describe the interaction of the photon with the two-level oscillators.

Generally, the effect of the environment on the behaviour of the system can be modelled through the interaction of the internal degrees of freedom with a bath. Taking into account different physical processes, the most general coupling is of the form

$$\begin{aligned} \hat{H}_{SB} = & \sum_k g_k (\psi^\dagger d_k + d_k^\dagger \psi) \\ & + \sum_{jk} \left[ b_j^\dagger a_j (g_{jk}^{\gamma+} c_{+,k}^\dagger + g_{jk}^{\gamma-} c_{-,k}) + \text{h.c.} \right] \\ & + \sum_{jk} \Gamma_{jk}^{(1)} (b_j^\dagger b_j + a_j^\dagger a_j) (c_{1,k}^\dagger + c_{1,k}) \\ & + \sum_{jk} \Gamma_{jk}^{(2)} (b_j^\dagger b_j - a_j^\dagger a_j) (c_{2,k}^\dagger + c_{2,k}), \quad (2) \end{aligned}$$

where

$$\begin{aligned} \hat{H}_B = & \sum_k \left[ \omega_k d_k^\dagger d_k + \omega_{+,k} c_{+,k}^\dagger c_{+,k} + \omega_{-,k} c_{-,k}^\dagger c_{-,k} \right. \\ & \left. + \omega_{1,k} c_{1,k}^\dagger c_{1,k} + \omega_{2,k} c_{2,k}^\dagger c_{2,k} \right] \end{aligned}$$

describes the Hamiltonian of the bath. Here the different modes  $k$  of the bath are indexed by (independent) Bosonic field operators  $d_k$ ,  $c_{+,k}$ ,  $c_{-,k}$ ,  $c_{1,k}$  and  $c_{2,k}$ . Here the first term in (2) describes the decay of the photon field from the cavity. Matrix elements  $g_{jk}^{\gamma+}$  describe the incoherent pumping of two-level oscillators, while the matrix elements  $g_{jk}^{\gamma-}$  contain all of the higher energy processes which destroy the electronic excitations such as the radiative decay into photon modes different from the cavity mode. Apart from their dephasing effect, together, these processes cause a flow of energy through the system. However, in the steady state, the total number of excitations

$$\hat{n}_{ex} = \psi^\dagger \psi + \frac{1}{2} \sum_j (b_j^\dagger b_j - a_j^\dagger a_j), \quad (3)$$

the sum of photons and excited two-level oscillators, is constant. Finally, the third and fourth terms describe all those lower energy dephasing processes, such as collisions

and interactions with phonons and impurities, which conserve the total number of excitations in the cavity. Such contributions can be divided into a part which act symmetrically ( $\Gamma^{(1)}$ ) or antisymmetrically ( $\Gamma^{(2)}$ ) on the upper and lower levels. Altogether these four terms contain all the essential mechanisms of decoherence.

To assimilate the effect of the different mechanisms of decoherence, we will find it useful both intuitively as well as technically (see later) to draw on an analogy between the Hamiltonian of the system and that of a superconductor [14,15]. Referring to the states indexed by the Fermionic operators  $b_j$  as ‘particle-like’, and those indexed by  $a_j$  as ‘hole-like’,  $\hat{H}_S$  can be interpreted as a BCS Hamiltonian for a superconductor with an imposed homogeneous ‘superconducting’ order parameter  $\psi$ . With this analogy, it is clear that the second and third terms of  $\hat{H}_{SB}$  (2) affect a mechanism of ‘pair-breaking’, while the fourth term is compatible with the symmetry of the Cooper pairs. The former act on the system as dynamically fluctuating magnetic impurities while the latter describe dynamical fluctuations of a normal non-magnetic potential providing only an inhomogeneous broadening of the energies.

When the pumping and photon decay rates are high, the system would be driven out of equilibrium. However, if the thermalisation rate is in excess of the speed at which the system is pumped, an equilibrium assumption can be justified. In this work we will limit our considerations to this regime focussing on the effect of decoherence on the equilibrium system. Choosing both the pumping and decay rates to be small — allowing thermal equilibration — their ratio can be used to fix the total excitation density  $n_{ex}$ . Nevertheless, within this quasi-equilibrium regime, both the third and fourth terms in (2) can, in fact, be arbitrary large since they do not couple to the total density  $n_{ex}$ . There is no restriction on the density of excitations nor on the decoherence rate.

Therefore, on this background, we will consider the total Hamiltonian

$$\hat{H} = \hat{H}_S + \hat{H}_{SB} + \hat{H}_B, \quad (4)$$

where

$$\begin{aligned} \hat{H}_{SB} = & \sum_{jk} \Gamma_{jk}^{(1)} (b_j^\dagger b_j + a_j^\dagger a_j) (c_{1,k}^\dagger + c_{1,k}) \\ & + \sum_{jk} \Gamma_{jk}^{(2)} (b_j^\dagger b_j - a_j^\dagger a_j) (c_{2,k}^\dagger + c_{2,k}), \quad (5) \end{aligned}$$

includes only the includes only the decoherence mechanisms which conserve  $n_{ex}$ , while

$$\hat{H}_B = \sum_{i=1,2} \sum_k \omega_{i,k} c_{ik}^\dagger c_{ik}.$$

Although, in general, the coupling constants  $\Gamma_{jk}^{(i)}$  can be site dependent, for simplicity, we will suppose that the modes of the bath couple with equal strength to the two-level systems setting  $\Gamma_{jk}^{(i)} \mapsto \Gamma_k^{(i)}$ . Similarly, in the following, we will assume that the coupling of the two-level

systems to the cavity photon is independent of the site index  $j$ ,  $g_j \mapsto g$ .

When the interactions between the environment and the system are large, the Hamiltonian above provides the basis of the standard theory of lasers (see, e.g., Refs. [10,11]). At the same time, if we set the coupling constants between the system and the environment to zero, the ground state of the Hamiltonian  $\hat{H}_S$  forms a polariton condensate. Thus by varying the magnitude of the coupling between the system and the baths the model provides the means to move smoothly between an isolated condensate and other phases driven by the decoherence. This provides a means to explore the stability of the polariton condensate to interactions with the outside world at a small coupling strength, and to establish the connection between polariton condensation and lasers as the decoherence is increased.

The standard assumption (which in many cases is physically correct) is that the environment leads to rapid dephasing of the exciton polarisation (i.e.  $T_2$  is very short). It is thus generally assumed that the polarisation is very small, and that the coherent photon field is the dominant order parameter. In such a case the baths can be averaged out before the exciton-photon interaction is studied. This in turn leads to the well-known quantum Maxwell-Bloch (Langevin) equations for the photon field and polarisation, essentially of the form

$$\frac{d}{dt}\langle a^\dagger b \rangle = i\langle [\hat{H}_S, a^\dagger b] \rangle - \frac{1}{T_2}\langle a^\dagger b \rangle \quad . \quad (6)$$

Crucially, Eq. (6) can be derived by assuming that the lifetime  $T_2$  for polarisation of a *single* two-level oscillator is the same as that of the macroscopic ensemble of two-level oscillators (which would correspond to introducing a separate bath for each two-level system). However, in general Eq. (6) is not correct [12]. When  $T_2$  is long, the macroscopic ensemble of two-level oscillators can exist in a collective state characterised by a large coherent polarisation, and the assumptions which lead to (6) cannot be justified. Moreover, the constant decay rate  $1/T_2$  in (6) is a critical parameter; even at arbitrarily small decoherence it leads to completely different solutions from those in the absence of an environment (as shown in Ref. [12]). This criticality is however unphysical and arises only due to approximations used in deriving the Langevin equations. In fact, this conclusion seems not to be widely appreciated. Indeed, in a relatively recent publication [13] similar decay constants in the equations of motion for the coherently driven excitonic insulator have been used, leading to the conclusion that the excitonic insulator phase cannot exist for an arbitrary small decoherence.

One can gain some physical insight into this problem by considering the evolution of the density of states: The ideal condensate has a gap in the density of states which would still be present for small decoherence. It is evident that the coherent fields in this regime cannot be damped

just by constant decay rates independent of frequency as there are no available states in which to decay. As the decoherence is increased this gap gets smaller and finally is completely suppressed causing the coherent fields to be strongly damped, as in lasers. In this regime Eq. (6) is perfectly valid. However to be able to study a crossover from the fully phase coherent polariton condensate to a laser one needs to include the environment in a self-consistent way in which the possible gap in excitation spectrum and a large polarisation would be taken into account.

The analogy between superconductivity and the excitonic insulator was first noticed and exploited in a pioneering work of Keldysh [14,15], and explored later by others [16,9]. The analogy between different types of decoherence processes acting on polariton condensate, and the problem of magnetic and potential impurities in superconductors suggests that similar methods to that used by Abrikosov and Gor'kov (AG) in their theory of gapless superconductivity [1] can be useful in studying the properties of polariton condensates in the presence of decoherence. This analogy is however not exact and we will discuss a few essential differences between our theory and the Abrikosov and Gor'kov approach at the end of Section III. An outline of the rest of the paper is as follows: In section III we provide details of the method in the path integral formulation. In section IV we discuss ground state properties of the system in the presence of two different types of dephasing while in section V we study the excitation spectrum and construct a phase diagram as a function of excitation density, pair-breaking decoherence strength and the inhomogeneous broadening of energy levels. In section VI we discuss a crossover between an isolated condensate and a laser and in section VII the magnitude of the energy gap. In section VIII we comment on the applicability of the model and the method presented in this work and indicate a few directions in which the model could be easily extended. Finally, in section IX we discuss recent experiments in the light of theoretical predictions presented in this work and in section X we briefly summarise the results.

### III. PATH INTEGRAL FORMULATION

To construct a theory of the coupled system, we will exploit an approach based on the coherent state path integral. As well as providing access to the mean-field equations of the system, such a framework provides the potential to explore the influence of fluctuation phenomena. Working in the grand canonical ensemble, a chemical potential  $\mu$  can be used to fix the total number of excitations  $n_{ex}$ . The quantum partition function of the system  $\mathcal{Z} = \text{Tr} e^{-\beta(\hat{H} - \mu \hat{n}_{ex})}$  can be expressed as a coherent state path integral over Fermionic and Bosonic fields,

$$\mathcal{Z} = \int D[\bar{\psi}, \psi] \prod_j D[\bar{\phi}_j, \phi_j] \prod_{k,i=1,2} D[\bar{c}_{i,k}, c_{i,k}] e^{-S} \quad (7)$$

As with the Hamiltonian, it is convenient to separate the total action as  $S = S_S + S_{SB} + S_B$  where

$$S_S = S_\psi - \int_0^\beta d\tau \sum_j \bar{\phi}_j \hat{G}_{0j}^{-1} \phi_j$$

with  $S_\psi = \int_0^\beta d\tau \bar{\psi}(\partial_\tau + \omega_c - \mu)\psi$  denotes the action of the internal electron and photon degrees of freedom of the system, while the action for the coupling of the system to the bath takes the form

$$S_{SB} = \int_0^\beta d\tau \sum_{i=1,2} \left[ \sum_k \bar{c}_{ik}(\partial_\tau + \omega_{ik})c_{ik} + \sum_k \Gamma_k^{(i)} \rho^{(i)}(\bar{c}_{i,k} + c_{i,k}) \right].$$

Combining the Fermionic fields of the two-level systems into a Nambu-like spinor,

$$\bar{\phi}_j = (\bar{b}_j \quad \bar{a}_j),$$

the bare Green function assumes the matrix form

$$\hat{G}_{0j}^{-1} = -\partial_\tau \sigma_0 - (\epsilon_j - \mu/2)\sigma_3 - g\bar{\psi}\sigma_- - g\psi\sigma_+.$$

where  $\sigma$  denote the Pauli spin matrices (with  $\sigma_0 \equiv \mathbb{1}$ ) which operate in the  $(b, a)$  space (hereafter, loosely referred to as the ‘particle/hole’ space). Finally, we have defined the symmetric and antisymmetric ‘densities’ according to the relation  $\rho(\tau)^{(1,2)} = \sum_j \bar{\phi}_j(\tau)\sigma_{(0,3)}\phi_j(\tau)$ .

Although a theory of the symmetric and antisymmetric processes can be developed in concert, for clarity we will present a detailed derivation of the action of the ‘pair-breaking’ decoherence processes imposed by  $\Gamma^{(1)}$ . Later, in Section III A, we will restore the decoherence processes affected by  $\Gamma^{(2)}$ . Thus, for now, we will use the following abbreviation  $\Gamma_k^{(1)} \mapsto \Gamma_k$  dropping the ‘channel’ index.

Being Gaussian in the Bosonic fields  $c_k$ , the degrees of freedom of the bath can be integrated out leading to an effective interaction of the two-level systems which takes the form  $\int D[\bar{c}_k, c_k] e^{-S_{SB}} = e^{-S'_{SB}}$ , where

$$S'_{SB} = \int_0^\beta d\tau d\tau' \rho(\tau) \sum_k \Gamma_k^2 D_k(\tau - \tau') \rho(\tau'), \quad (8)$$

with  $\hat{D}_k^{-1} = -\partial_\tau - \omega_k$  representing the free propagator of the environment. Transforming (8) to the Fourier Matsubara frequency representation, and summing over the internal degrees of freedom of the bath,

$$-\sum_k \Gamma_k^2 D_k(i\nu_n) = f_\Gamma(i\nu_n), \quad (9)$$

where  $D_k^{-1}(\nu_n) = i\nu_n - \omega_k$  and  $\nu_n = 2\pi n/\beta$ , the induced interaction assumes the form

$$S'_{SB} = -\sum_{\nu_n} f_\Gamma(i\nu_n) \rho(i\nu_n) \rho(-i\nu_n) \\ = \int_0^\beta d\tau d\tau' f_\Gamma(\tau - \tau') \sum_{jj'} \text{Tr} \phi_j(\tau) \otimes \bar{\phi}_{j'}(\tau') \phi_{j'}(\tau') \otimes \bar{\phi}_j(\tau).$$

In particular, it can be seen explicitly that the interaction with the environment introduces an effective quartic interaction between the *different* two-level systems. This contrasts with the Maxwell-Bloch equations (6) from which one can infer only a lifetime for excitations [12].

To develop a mean-field theory of the coupled system, it is helpful to affect a Hubbard-Stratonovich decoupling of the interaction. Introducing the  $2 \times 2$  component matrix field  $Q_{jj'}(\tau, \tau')$ , which inherits the symmetry of the dyadic product  $\phi_j(\tau) \otimes \phi_{j'}(\tau')$ , the interaction generated by the bath can be decoupled as

$$e^{-S'_{SB}} = \int DQ e^{-S_Q} \\ \times \exp \left[ \int_0^\beta d\tau d\tau' f_\Gamma(\tau - \tau') \sum_{jj'} \bar{\phi}_j(\tau) Q_{jj'}(\tau, \tau') \phi_{j'}(\tau') \right],$$

where

$$S_Q = \int_0^\beta d\tau d\tau' \sum_{jj'} f_\Gamma(\tau - \tau') \text{Tr} Q_{jj'}(\tau, \tau') Q_{j'j}(\tau', \tau)$$

with trace taken in the particle-hole space. Combined with  $S_S$ , an integration over the Fermionic degrees of freedom  $\phi$  obtains the quantum partition function

$$\mathcal{Z} = \int D[\bar{\psi}, \psi] \int DQ e^{-S}. \quad (10)$$

where  $S = S_Q + S_\psi - \text{Tr} \ln \hat{G}^{-1}$ ,

$$G_{jj'}^{-1}(\tau, \tau') = G_{0j}^{-1} \delta_{jj'} \delta(\tau - \tau') - f_\Gamma(\tau - \tau') Q_{jj'}(\tau, \tau'). \quad (11)$$

and the trace now runs over time and site indices as well as the particle/hole space. At this level, the analysis is exact.

### A. Saddle-point equations

To develop the quantum partition function, further progress is possible only within a saddle-point approximation. Varying the action with respect to  $Q$ , one finds that each electronic excitation is coupled to the average field created by all of the other excitations. In this sense, the saddle-point analysis corresponds to a mean-field treatment of the interaction between electronic excitations. This analysis becomes exact when there is a large number of electronic excitations coupled to a small number of field modes, since the fluctuations of the field are then negligible [9]. The mean-field treatment of the interaction becomes exact in the thermodynamic limit

when  $N \rightarrow \infty$ . The fluctuations above mean-field are of the order of  $1/\sqrt{N}$ .

In the saddle-point approximation, it is assumed that the dominant contribution to the quantum partition function (7) arises from those configurations  $\psi$  and  $Q$  which minimise the total action. Varying the action  $S$  with respect to  $Q$  one obtains the matrix equation

$$Q_{jj'}(\tau, \tau') = \frac{1}{2} G_{jj'}(\tau, \tau'), \quad (12)$$

while varying with respect to  $\bar{\psi}$ , the saddle-point equation takes the form

$$(\partial_\tau + \omega_c - \mu)\psi(\tau) = \sum_j g \text{Tr} G_{jj}(\tau, \tau) \sigma_-. \quad (13)$$

Maintaining the analogy with the superconductor, the first equation which identifies  $Q$  as the self-energy, describes the self-consistent Born approximation for the Green function, while the second equation represents the gap equation for the superconducting order parameter. Substituting Eq. (12) into (11) the saddle-point equation assumes the form of a Dyson equation

$$G_{jj'}^{-1}(\tau, \tau') = G_{0j}^{-1}(\tau, \tau') \delta_{jj'} - \Sigma_{jj'}(\tau, \tau'), \quad (14)$$

where

$$\Sigma_{jj'}(\tau, \tau') = \frac{1}{2} f_\Gamma(\tau - \tau') G_{jj'}(\tau, \tau')$$

denotes the self-energy

Until now, we have focussed on the impact of the ‘pair-breaking’ perturbation affected by the matrix elements  $\Gamma^{(1)}$ . Consideration of the symmetric perturbation  $\Gamma^{(2)}$  follows straightforwardly. In doing so, it may be confirmed that the structure of the saddle-point equations are maintained while the self-energy takes the form

$$\Sigma_{jj'}(\tau, \tau') = \frac{1}{2} f_\Gamma(\tau - \tau') \sigma_3 G_{jj'}(\tau, \tau') \sigma_3$$

In steady state one expects the solution of the saddle-point equations to depend only on  $\tau - \tau'$ . In this case, a transformation to Matsubara frequencies leads to the relation

$$\Sigma(i\nu_n) = \frac{1}{2} \sum_{\nu'_n} f_\Gamma(i\nu'_n) G(i\nu_n - i\nu'_n). \quad (15)$$

Generally, the solution of the saddle-point equation depends sensitively on the particular spectrum of decoherence  $f_\Gamma$  and must be determined self-consistently. However, an explicit solution to the saddle-point equation can be established in various limits.

Generally, in order to determine  $f_\Gamma$  from Eq. (9) one can assume that coupling constants of the system to the bath  $\Gamma_k$ , as well as the bath density of states  $N(\omega_k)$ , are continuous functions of frequency. In this case, one can

replace the summation over  $k$  with an integral over  $\omega_k$  ( $\Gamma_k \mapsto \Gamma(\omega_k)$ ,  $\sum_k \mapsto \int d\omega_k N_k(\omega_k)$ ) whereupon

$$f_\Gamma(i\nu_n) = \int d\omega_k \frac{N_k(\omega_k) \Gamma^2(\omega_k)}{-i\nu_n - \omega_k}.$$

Now, in general  $f_\Gamma$  will exhibit a particular frequency dependence determined by the density of states  $N(\omega_k)$  of the bath and coupling constant  $\Gamma(\omega_k)$ . However two special cases present themselves: Firstly, if we assume that both  $\Gamma(\omega_k)$  and  $N(\omega_k)$  are largely independent of frequency over a wide range, one finds  $f_\Gamma(i\nu_n) = i2\pi\Gamma^2 N$ . This corresponds to a Markovian approximation to the bath in which  $f_\Gamma(\tau) = i2\gamma^2\delta(\tau)$ . In the second limit, if one assumes that the matrix elements and density of states are concentrated at zero frequency, one has  $f_\Gamma(i\nu_n) = 2\gamma^2\delta_{\nu_n,0}$ . Here, in the static limit,  $f_\Gamma(\tau) = 2\gamma^2$  is *real*. Applied to the self-energy, the static limit leads to

$$\Sigma_{jj'}(i\nu_n) = \gamma^2 G_{jj'}(i\nu_n),$$

while, in the Markovian approximation,

$$\Sigma_{jj'}(\tau, \tau) = i\gamma^2 G_{jj'}(\tau, \tau),$$

(similarly for the perturbation  $\Gamma^{(2)}$ ). In these two limiting cases, the saddle-point equations admit a straightforward analytical solution. Here we present a detailed analysis for the static limit.

Noting that photon field in the gap equation (13) couples only to the diagonal elements of the Green function,  $G_{jj}$ , this suggests a mean-field Ansatz in which the matrix elements off diagonal in the  $j$  space are taken to be zero, while the only time dependence of the field is associated with oscillation at the chemical potential,  $\mu$ . In this case, the coupled equations (13), (14) can now be solved.

To simplify the algebra we employ a similar mathematical trick to that used by Abrikosov and Gor'kov in their theory of gapless superconductors. Since the overall phase of a coherent state is arbitrary, we can choose the mean-field  $\langle\psi\rangle$  to be real and present the total Green function  $G$  (14) in the same form as the zero-order Green function  $G_0$ ,

$$G_{jj}^{-1}(i\nu_n) = -i\tilde{\nu}_{j,n} - (\tilde{\epsilon}_j - \mu/2)\sigma_3 - g\langle\tilde{\psi}_j\rangle\sigma_1, \quad (16)$$

using the frequency dependent, renormalised  $\tilde{\nu}_{j,n}$ ,  $\tilde{\epsilon}_j$  and  $\langle\tilde{\psi}_j\rangle$ . Comparing (14) with (16) we obtain for both type 1 and type 2 decoherence three equations determining the renormalised frequency, energy and coherent photon field

$$\tilde{\nu}_{j,n} = \nu_n - \gamma_{1,2}^2 \frac{\tilde{\nu}_{j,n}}{\tilde{\nu}_{j,n}^2 + (\tilde{\epsilon}_j - \mu/2)^2 + g^2\langle\tilde{\psi}_j\rangle^2}, \quad (17)$$

$$\tilde{\epsilon}_j = \epsilon_j + \gamma_{1,2}^2 \frac{\tilde{\epsilon}_j}{\tilde{\nu}_{j,n}^2 + (\tilde{\epsilon}_j - \mu/2)^2 + g^2\langle\tilde{\psi}_j\rangle^2}, \quad (18)$$

$$\langle\tilde{\psi}_j\rangle = \langle\psi\rangle \pm \gamma_{1,2}^2 \frac{g_j\langle\tilde{\psi}_j\rangle}{\tilde{\nu}_{j,n}^2 + (\tilde{\epsilon}_j - \mu/2)^2 + g^2\langle\tilde{\psi}_j\rangle^2}. \quad (19)$$

while the gap equation (13) takes the form

$$\langle \psi \rangle = \frac{g}{2(\omega_c - \mu)} \sum_j \text{Tr} G_{jj} \sigma_1. \quad (20)$$

The average coherent polarisation of the medium can be determined from the off-diagonal part of the Green's function  $G$  (16)

$$\begin{aligned} \frac{1}{N} \langle \sum_j a_j^\dagger b_j \rangle &= \langle P \rangle \\ &= -\beta^{-1} \sum_{\nu_n, j} \frac{g \langle \tilde{\psi}_j \rangle}{\tilde{\nu}_{j,n}^2 + (\tilde{\epsilon}_j - \mu/2)^2 + g^2 \langle \tilde{\psi}_j \rangle^2}. \end{aligned} \quad (21)$$

Thus, at the mean-field level, we can see from Eqs. (20) and (21) that the two order parameters, the coherent polarisation and the coherent photon field, are coupled according to the relation

$$\langle \psi \rangle = -\frac{g}{\omega_c - \mu} \langle P \rangle. \quad (22)$$

---


$$\langle \tilde{\psi}_j \rangle = \frac{\langle \psi \rangle}{2} + \frac{\sqrt{2} \langle \psi \rangle}{4E_j} \sqrt{E_j^2 - 4\gamma_1^2 - \nu_n^2 + \sqrt{-16\gamma_1^2 E_j^2 + (E_j^2 + 4\gamma_1^2 + \nu_n^2)^2}}, \quad (24)$$

and

$$\tilde{\nu}_{j,n} = \frac{\nu_n \langle \tilde{\psi}_j \rangle}{2 \langle \tilde{\psi}_j \rangle - \langle \psi \rangle}, \quad (25)$$

$$\tilde{\epsilon}_j = \frac{\epsilon_j \langle \tilde{\psi}_j \rangle}{\langle \psi \rangle}, \quad (26)$$

---


$$\langle \tilde{\psi}_j \rangle = \frac{\langle \psi \rangle}{2} +$$

$$\frac{\sqrt{2} \langle \psi \rangle}{4(\nu_n^2 + g^2 \langle \psi \rangle^2)} \sqrt{E_j^2 - 2(\epsilon_j - \mu/2)^2 + 4\gamma_1^2 - \nu_n^2 + \sqrt{16\gamma_2^2(\nu_n^2 + g^2 \langle \psi \rangle^2) + (E_j^2 - 4\gamma_1^2 + \nu_n^2)^2}}, \quad (27)$$

and

$$\tilde{\nu}_{j,n} = \frac{\nu_n \langle \tilde{\psi}_j \rangle}{\langle \psi \rangle}, \quad (28)$$

$$\tilde{\epsilon}_j = \frac{\epsilon_j \langle \tilde{\psi}_j \rangle}{2 \langle \tilde{\psi}_j \rangle - \langle \psi \rangle}, \quad (29)$$

where for both cases

$$E_j = \sqrt{(\epsilon_j - \mu/2)^2 + g^2 \langle \psi \rangle^2}. \quad (30)$$

Substituting Eqs. (24)-(26) or (27)-(29) into Eq. (21), summing over the Matsubara frequencies, and using Eq. (22) we can determine the ground state coherent

The ratio between the two order parameters is determined by the chemical potential, which in the steady state can be calculated from Eq. (3).

The number of electronic excitations, referred to later as inversion, can be obtained from the diagonal elements of the Green's function

$$\begin{aligned} \frac{1}{2} \langle \sum_j (b_j^\dagger b_j - a_j^\dagger a_j) \rangle \\ = -\beta^{-1} \sum_{\nu_n, j} \frac{2(\tilde{\epsilon}_j - \mu/2)}{\tilde{\nu}_{j,n}^2 + (\tilde{\epsilon}_j - \mu/2)^2 + g^2 \langle \tilde{\psi}_j \rangle^2}. \end{aligned} \quad (23)$$

Using Eqs. (17)-(19) we can determine the renormalised parameters  $\tilde{\nu}_{j,n}$ ,  $\tilde{\epsilon}_j$  and  $\langle \tilde{\psi}_j \rangle$  as a functions of the bare parameters  $\nu_n$ ,  $\epsilon_j$ ,  $\langle \psi \rangle$  and  $\gamma$ . In the case of type 1 decoherence processes we obtain

---

while for the type 2 decoherence processes we have

---

polarisation  $\langle P \rangle$  and the coherent photon field  $\langle \psi \rangle$  as functions of the system parameters  $\epsilon$ ,  $\omega_c$ , decoherence parameter  $\gamma_{1,2}$  and chemical potential  $\mu$ . The chemical potential can be then obtained from Eq. (3). The integrals over the Matsubara frequencies at zero temperature in (21) and (23) as well as the determination of the chemical potential from (3) have to be performed numerically.

## B. Density of states

The excitation spectrum, i.e the density of states, can be obtained from the diagonal part of the Green function on the real frequency axis. Considering the analyt-

ical continuation of  $G_{jj}(i\nu_n) \rightarrow \bar{G}_{jj}(\nu)$ , where  $\nu_n$  and  $\nu$  are the Matsubara and the real frequencies respectively, and thus using the usual substitution  $i\nu_n \rightarrow -\nu + i\delta$ , we obtain the relationship between the Green function  $G_{jj}(i\nu_n)$  and the density of states  $A(\nu)$

$$A(\nu) = \sum_j \lim_{\delta \rightarrow 0^+} \text{Im} G_{jj}(-\nu + i\delta + \mu), \quad (31)$$

which has the following form

$$A(\nu) = \sum_j \text{Im} \frac{\tilde{\nu}_j + (\tilde{\epsilon}_j - \mu/2)}{\tilde{\nu}_j^2 + (\tilde{\epsilon}_j - \mu/2)^2 + g^2 \langle \tilde{\psi}_j \rangle^2}. \quad (32)$$

Generally,  $\tilde{\nu}_j$ ,  $\tilde{\epsilon}_j$  and  $\langle \tilde{\psi}_j \rangle$  are functions of  $\nu$ ,  $\epsilon_j$ ,  $\langle \psi \rangle$  and  $\gamma$  which can be determined from Eqs. (24)-(26) or (27)-(29) by the following substitution  $i\nu_n \rightarrow -\nu + i\delta$ . It can be shown from Eq. (32) that the system of two-level oscillators with uniform energies,  $\epsilon_j = \epsilon$ , in the presence of the type 1 processes has a gap,  $\Delta$ , in the density of states of magnitude

$$\Delta = 2\sqrt{(\epsilon - \mu/2)^2 + g^2 \langle \psi \rangle^2} - 4\gamma_1. \quad (33)$$

At very high excitation densities the gap is proportional to the coherent field amplitude  $\Delta \approx 2g\langle \psi \rangle - 4\gamma_1$ . At very low excitation densities, when  $\langle \psi \rangle \rightarrow 0$ , we recover conventional polaritons for which the chemical potential is  $2\epsilon - \mu \rightarrow g$  and the gap  $\Delta \rightarrow g - 4\gamma_1$ .

The major difference between this work and the AG theory [1] is that the system studied here has two order parameters connected through the chemical potential which needs to be determined. We use a different form of the density of states for the two-level oscillators than in their theory. Instead of a flat distribution of energies from  $-\infty$  to  $+\infty$  used in the AG method we first perform the calculations for the degenerate case where all two-level oscillators have the same energy  $\epsilon$  and then we use a realistic Gaussian distribution of energies, present in the real microcavities. To account for these differences we need to include the additional, third equation for renormalised  $\tilde{\epsilon}$  not present in the original Abrikosov and Gor'kov method and the constraint equation for  $n_{ex}$ . In the Abrikosov and Gor'kov theory they consider free propagating electrons with momentum  $\mathbf{k}$  over which all the summations are performed. In our model of the localised two-level systems the summations are performed over the sites where the two-level oscillators can be present. Dynamic impurities can easily be included in our formalism.

To perform the calculations we rescale the coherent fields by  $\sqrt{N}$  and consequently the inversion and the number of excitations by  $N$  introducing the excitation density  $\rho_{ex} = n_{ex}/N$ . In this terminology the minimum  $\rho_{ex} = -0.5$  corresponds to no photons and no electronic excitations in the system. The condition  $\rho_{ex} = 0.5$  in the absence of photons would correspond to all two-level oscillators in excited states, thus to the maximum inversion.

We calculate first the ground state coherent field  $\langle \psi \rangle$ , the coherent polarisation  $\langle P \rangle$ , the inversion and the chemical potential as functions of the decoherence strength  $\gamma$  and the excitation density  $\rho_{ex}$  for different distributions of excitonic energies. Then we study the excitation spectrum of the system for different regimes. The ground state properties and the excitation spectrum allow us to obtain a phase diagram for different excitation densities and decoherence strengths. We consider the influence of both type 1 and type 2 decoherence processes as well as inhomogeneous broadening of exciton energies.

#### IV. THE GROUND STATE — COHERENT FIELDS

##### A. Type 1 (Pair-Breaking) Decoherence Processes

To examine the ground state properties of the system in the presence of the type 1 decoherence processes we study the mean value of the annihilation operator of the field and the polarisation. This mean is non-zero only in a coherent state. Figure 2 (upper panel) shows the behaviour of the coherent part of the photon field  $\langle \psi \rangle$  as the decoherence strength  $\gamma$  is changed for different excitation densities  $\rho_{ex}$  and different inhomogeneous broadenings of exciton energies.

For small values of  $\gamma/g$ , up to some critical value  $\gamma_{C1}$ ,  $\langle \psi \rangle$  is practically unchanged while for  $\gamma/g > \gamma_{C1}$  the coherent field is damped quite rapidly with increasing decoherence. This critical value of the decoherence strength,  $\gamma_{C1}$  is proportional to  $\rho_{ex}$ , suggesting that for higher excitation densities the system is more resistant to dephasing. At low excitation densities, where  $\rho_{ex} < 0$ , there is a second critical value of the decoherence strength,  $\gamma_{C2}$ , where both coherent fields are sharply damped to zero. As the excitation density is increased, precisely at  $\rho_{ex} = 0$ ,  $\gamma_{C2}$  diverges and does not exist for  $\rho_{ex} > 0$  — coherent fields although reduced are never completely suppressed.

The behaviour of the electronic inversion, which is a measure of the excitonic density given by Eq. (23), is presented in Fig. 2 (middle panel). In our terminology an inversion of -0.5 corresponds to no excitons while an inversion equal to zero means that the excitonic system is half occupied (roughly 0.5 per Bohr radius in a model where double occupation of excitonic sites is not allowed). Inversion of 0.5 would then correspond to 1 exciton per Bohr radius. In this region of the decoherence strength where  $\langle \psi \rangle$  is damped, the inversion increases. At low excitation densities ( $\rho_{ex} < 0$ ) the inversion approaches  $\rho_{ex}$  for  $\gamma/g = \gamma_{C2}$  and stays constant as  $\gamma$  is further increased. At high excitation densities ( $\rho_{ex} > 0$ ) the inversion asymptotically approaches zero with increasing dephasing. The maximum value of electronic inversion, for any exciton density and decoherence strength, is zero, which corresponds to a half filled excitonic system. This



is a consequence of our assumption of thermal equilibrium in the exciton-photon system.

The ratio of coherent polarisation to coherent field  $\langle P \rangle / \langle \psi \rangle$  is presented in Fig. 2 (lower panel). For an isolated system, where  $\gamma = 0$ , this ratio depends on the excitation density. The condensate becomes more photon like as  $\rho_{ex}$  is increased due to the phase space filling effect. For finite  $\gamma$ , at a given excitation density, this ratio decreases with increasing  $\gamma$  meaning that the coherent polarisation is more heavily damped than the coherent photon field by the type 1 decoherence processes. At  $\rho_{ex} < 0$  this ratio becomes undefined for  $\gamma/g > \gamma_{C2}$  when both coherent fields vanish.

In order to study the system of realistic, inhomogeneously broadened two-level oscillators we have replaced the summations over sites with integrals over the energy distribution. We have assumed this distribution to be a Gaussian with mean  $\epsilon_0$  and variance  $\sigma$ . Our results, presented as dashed and dashed-dotted lines in Fig 2 show that a Gaussian broadening of energies does not make any qualitative difference to the degenerate case. The coherent fields and the critical values of decoherence strength,  $\gamma_{C1}$  and  $\gamma_{C2}$  are, as expected, slightly smaller than in the degenerate case but all the regimes are analogous.

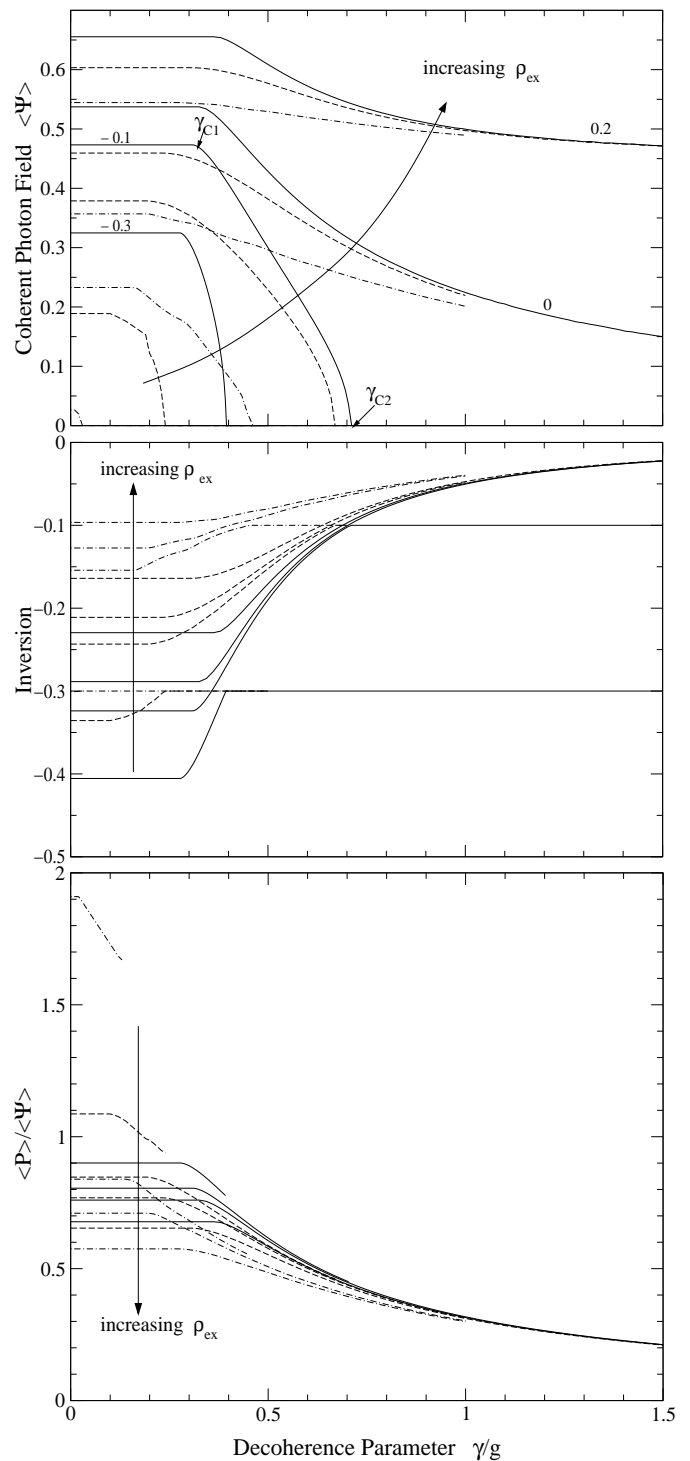


FIG. 2. Coherent photon field  $\langle \psi \rangle$  (upper panel), inversion (middle panel) and ratio between coherent photon field and coherent polarisation  $\langle P \rangle / \langle \psi \rangle$  (lower panel) as functions of the pair-breaking decoherence strength,  $\gamma/g$  for different excitation densities,  $\rho_{ex}$  and variances of inhomogeneous broadening  $\sigma = 0$  (solid lines),  $\sigma = 0.5$  (dashed lines) and  $\sigma = 1.0$  (dotted lines).

### B. Type 2 (Non-Pair-Breaking) Decoherence Processes

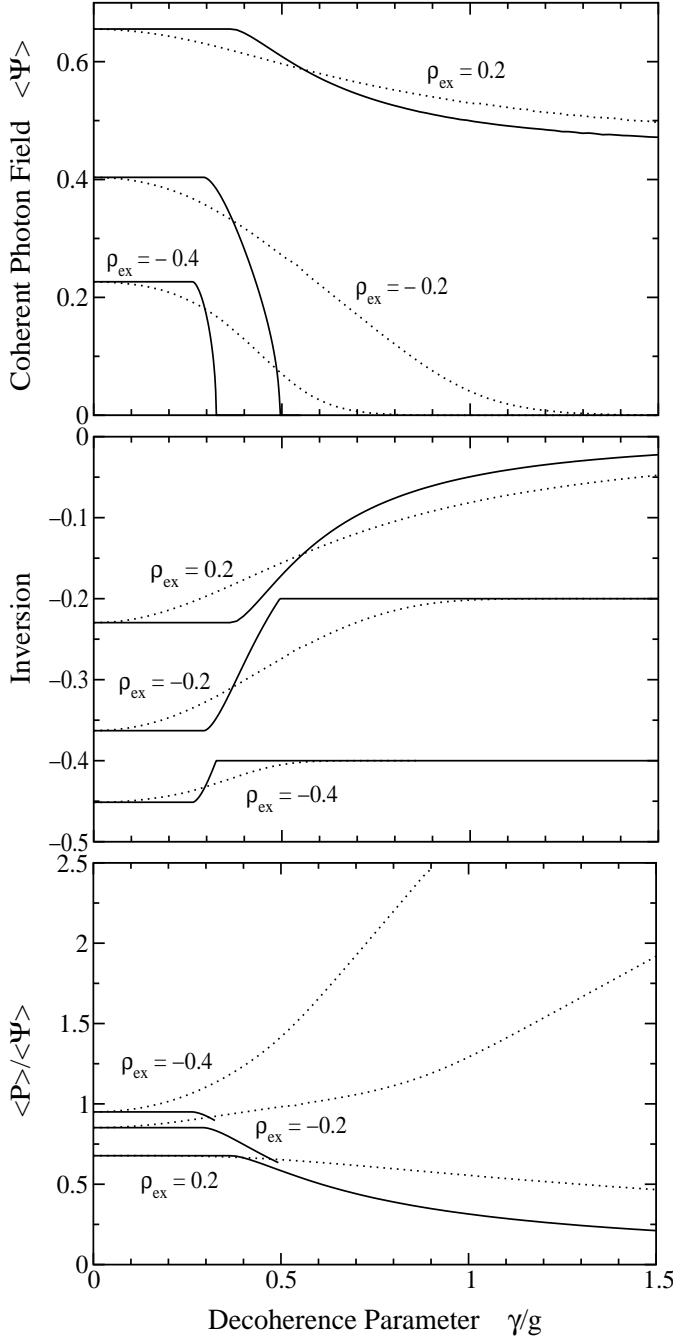


FIG. 3. Comparison between the influence of a pair-breaking (solid line) and a non-pair-breaking (dotted line) decoherence processes on  $\langle \psi \rangle$  (upper panel), inversion (middle panel) and  $\langle P \rangle / \langle \psi \rangle$  (lower panel) for three different values of  $\rho_{ex}$ .

We now repeat the analysis for type 2 decoherence processes (5), which act in an exactly the same way on the

upper and the lower levels of the two-level oscillator. Recall that such processes mirror the effects of non-magnetic impurities in the superconductor.

In Fig. 3 we present for comparison the coherent photon field (upper panel), the inversion (middle panel), and the ratio between the coherent polarisation and the coherent photon field (lower panel) in the presence of the type 1 (solid line) and the type 2 (dotted line) decoherence processes for three excitation densities  $\rho_{ex} = -0.4$ ,  $\rho_{ex} = -0.2$  and  $\rho_{ex} = 0.2$ . It is evident that the singular behaviour at  $\gamma_{C1}$  and  $\gamma_{C2}$  discussed for the type 1 decoherence processes is not present for the case of the type 2 processes. With an increase of the decoherence strength from zero the coherent fields are slightly reduced and they slowly decrease, asymptotically approaching zero at low excitation densities ( $\rho_{ex} < 0$ ) or a constant value at high densities ( $\rho_{ex} > 0$ ). Although both coherent fields are reduced the behaviour of their ratio strongly depends on the excitation density. We will show in Section VB that the type 2 processes give rise to the broadening of energies and then the behaviour of the ratio  $\langle P \rangle / \langle \psi \rangle$  depends on the position of the chemical potential with respect to the energy distribution. The type 2 processes can make the condensate more photon or more exciton like depending on the parameters of the system. The two different cases are presented in Fig. 3 (lower panel).

### V. EXCITATION SPECTRUM AND THE PHASE DIAGRAM

To understand the behaviour of the coherent fields we study the excitation spectrum of the system in different regimes. The density of states of the system with uniform energy distribution for six different values of  $\gamma$  at low excitation density  $\rho_{ex} = -0.4$  is presented in Fig. 4 while at high excitation density  $\rho_{ex} = -0.2$  in Fig. 5.

#### A. Type 1 (Pair-Breaking) Decoherence Processes

In the absence of decoherence (Fig. 4 a and 5 a) we have two sharp peaks at two quasi-particle energies,  $\pm E$ , given by equation (30) for the degenerate case ( $E_j = E$ ). As  $\gamma$  increases these two peaks broaden, which causes a decrease in the magnitude of the energy gap (Fig. 4 b, c and 5 b, c, d). The magnitude of the energy gap in the degenerate case is equal to  $2E - 4\gamma$ , which is given in more detail in equation (33). Finally, precisely at  $\gamma_{C1}$  (shown in Fig. 2), these two broadened peaks join together and the gap closes (Fig. 4 d and 5 e). When the decoherence strength is increased further (Fig. 4 e) these two peaks overlap more and the shape of the gapless density of states changes. For  $\gamma/g > \gamma_{C2}$  at low densities the coherent fields are suppressed, thus Fig 4 f shows the normal state density of states in the absence of coherence. Finally, at high densities (Fig. 5 f), as one would expect

for a laser system, the coherent field is present without a sign of a gap.

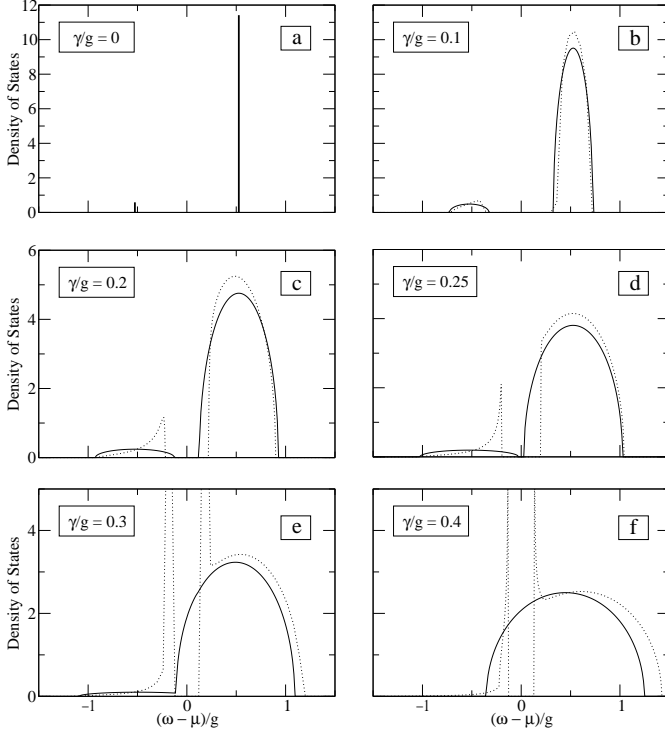


FIG. 4. Density of states for  $\rho_{ex} = -0.4$  and different decoherence strengths,  $\gamma/g$  for a pair-breaking (solid line) and a non-pair-breaking (dotted line) decoherence processes.

Fig 6 shows the density of states for the system of the inhomogeneously broadened two-level oscillators with standard deviation  $\sigma = 0.5g$  for different values of the type 1 decoherence strength at two different excitation densities. The broadening of the density of states and the suppression of the energy gap can be observed as  $\gamma$  is increased. The last curve in the Fig 6 (left panel) shows the normal state density where the coherent fields are suppressed. In the Fig 6 (right panel) where the coherent fields are present for all the values of  $\gamma$  the last curve has no sign of a gap.

There are clearly three different phases depending on the decoherence strength,  $\gamma$  (homogeneous broadening), inhomogeneous broadening,  $\sigma$  and the excitation density  $\rho_{ex}$ . In the Fig. 7 we present a phase diagram for the system. The phase boundaries are defined by  $\gamma_{C1}$  and  $\gamma_{C2}$  for different values of  $\rho_{ex}$  and  $\sigma$ .

Below the white surface, for small decoherence, we have a phase in which both coherent fields and an energy gap in the density of states are present. In this region coherent fields are protected by the energy gap and remain practically unchanged while the energy gap narrows as the decoherence is increased. At low densities within this phase we have a BEC of polaritons with the electronic and photonic parts comparable in size. At

high densities we have a BCS-type of condensate with photon component increasing with the excitation density. Despite the predominantly photon-like character of this phase at very high densities, the coherence of the medium is still large and this phase can be distinguished from a laser by the presence of a gap in the density of states (Fig 6 - right panel). The crossover between high and low densities is a smooth evolution and there are no rapid phase transitions.

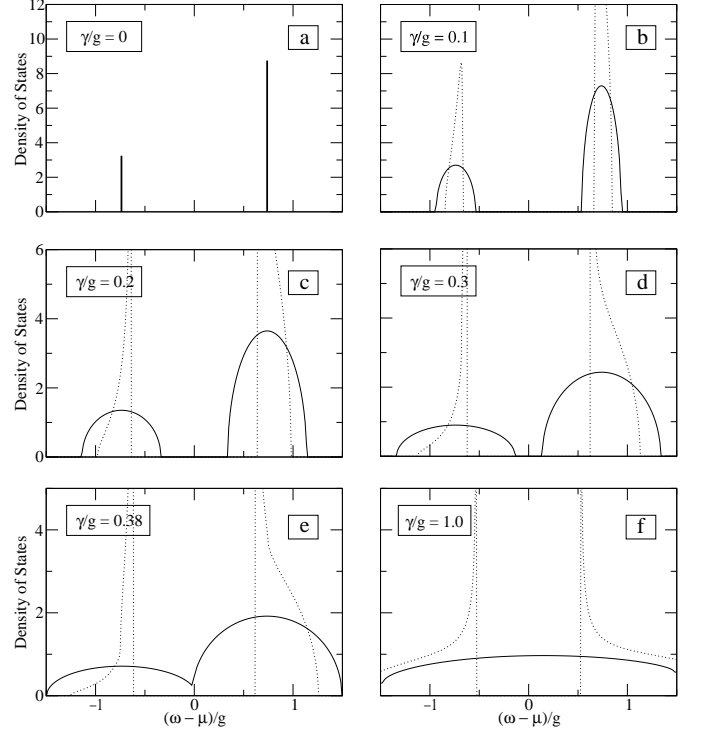


FIG. 5. Density of states for  $\rho_{ex} = 0.2$  and different decoherence strengths,  $\gamma/g$  for a pair-breaking (solid line) and a non-pair-breaking (dotted line) decoherence processes.

Inhomogeneous broadening has some influence on this phase mainly at low excitation densities. The critical decoherence  $\gamma_{C1}$ , which defines a boundary between gapped and gapless phases, decreases with an increase in the inhomogeneous broadening  $\sigma$ . At high excitation densities inhomogeneous broadening has very weak influence on the system.

Between the white and gray surfaces there is a phase where the coherent fields are present without an energy gap in the density of states. This phase exists for all values of the decoherence parameter at high excitation densities  $\rho_{ex} > 0$ . The coherent fields are no longer protected by the gap and get reduced as the decoherence is increased. The coherent polarisation is more heavily damped than the coherent field. Within this phase we have at low densities a gapless, light-matter condensate, analogous to gapless superconductivity, whilst at very high densities we have essentially the laser system. Fi-

nally, above the dashed line there is a phase where the

coherent fields are completely suppressed.

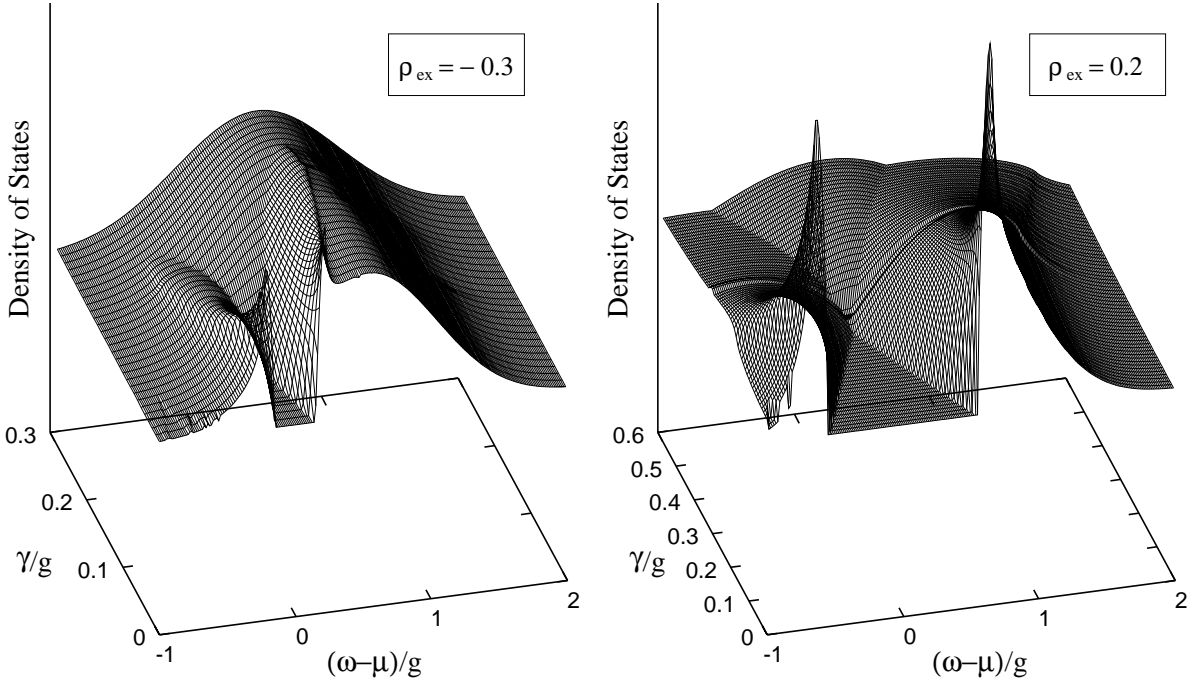


FIG. 6. Density of states for the Gaussian broaden case with  $\sigma = 0.5$  for different values of the pair-breaking decoherence strength at  $\rho_{ex} = -0.3$  (left panel) and  $\rho_{ex} = 0.2$  (right panel).

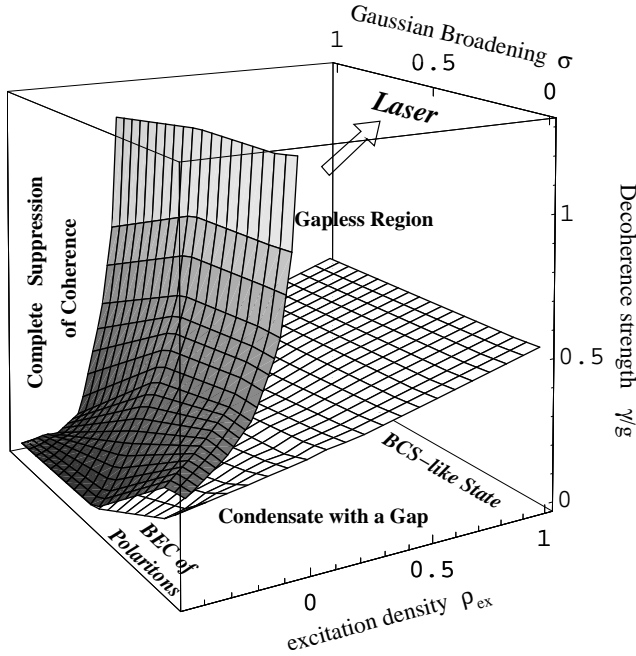


FIG. 7. Phase diagram. The phase boundaries  $\gamma_{C1}$  and  $\gamma_{C2}$  as marked in Fig 2.

### B. Type 2 (Non-Pair-Breaking) Decoherence Processes

The density of states in the presence of type 2 processes is shown in Figs 4 and 5 (dotted lines). It can be seen that, although the two quasiparticle peaks get very broad, the gap is only slightly affected by the type 2 processes and is always present. Even for much larger values of  $\gamma$  than presented in Figs 4 and 5 the gap is not suppressed. The gap in the density of states is present until the coherent fields get completely suppressed. At high excitation densities ( $\rho_{ex} > 0$ ) coherent fields are always present and thus the density of states will have a gap for all values of the decoherence strength.

The type 2 processes give a similar effect as the inhomogeneous broadening of energy levels in the case of an isolated system (see Ref. [9]). The difference is that the density of states in the presence of the type 2 processes has sharp boundaries. This is a result of the method which is used to perform the calculations. It can be seen that if the bath operators for the type 2 processes,  $c_2$ 's in

expression (5), were just numbers, this term could have been included into the second term in equation (1) and would have just given a random  $\epsilon_i$ . In our calculations the  $c_2$ 's are operators and we use a self-consistent Born approximation, which is not exact, and does not correctly reproduce the tail of the distribution. Thus, because of the way the calculations are done, the density of states produced always has sharp boundaries.

In the Abrikosov and Gor'kov theory, due to the flat density of states used in the calculations, the non-magnetic impurities do not influence the superconducting state at all. In the case of degenerate or realistic, Gaussian distributed energies of the two level oscillators the type 2 processes have some quantitative influence on the coherent fields and the gap but cannot cause any phase transitions.

## VI. CROSSOVER TO LASER

The features of the second phase (between the white and the gray surfaces) in Fig. 7 at high  $\rho_{ex}$  are essentially the same as those of the laser system. The laser operates in the regime of a very strong decoherence, comparable with the light-matter interaction itself. In the presence of such a large decoherence laser action can be observed only for a sufficiently large excitation density. The coherent polarisation in a laser system is much more heavily damped than the photon field and the gap in the density of states is not observed. Thus the laser is a regime of our system for very large  $\rho_{ex}$  and  $\gamma$ .

Laser theories, due to the approximations on which they are based, can only be valid in a regime where the gap in the density of states is suppressed and thus for a large decoherence. At the time when these theories were proposed they were deemed sufficient as most lasers operate in such a regime. Miniaturisation and improvements in the quality of optical cavities in recent years can lead to a large suppression of decoherence in laser media. For small decoherence and very small pumping in comparison to decay processes, when  $\rho_{ex}$  is much smaller than 0, the laser theories would predict a lack of coherence while the real ground state of the system would be a more matter-like condensate. Thus an extension of laser theories to account for the gap in the excitation spectrum and coherence in a media is necessary. In our theory the laser emerges from the polariton condensate at high densities when the gap in the density of states closes for large decoherence and thus is analogous to a gapless superconductor.

When both the gap and the coherence in a media are taken into account, in contrast to a traditional laser, the coherent photon field can be present without the population inversion in the media. The polariton condensate is thus an example of a laser without inversion.

However, it has to be pointed out that there is no formal distinction between a laser and a Bose condensate of

polaritons. In the laser, coherence in the medium (manifested by the coherent polarisation) although small, is not completely suppressed so the laser can be seen as a gapless condensate with a more photon-like character. One of the possible distinctions between BEC and laser could be an existence of an energy gap in the excitation spectrum.

## VII. THE GAP

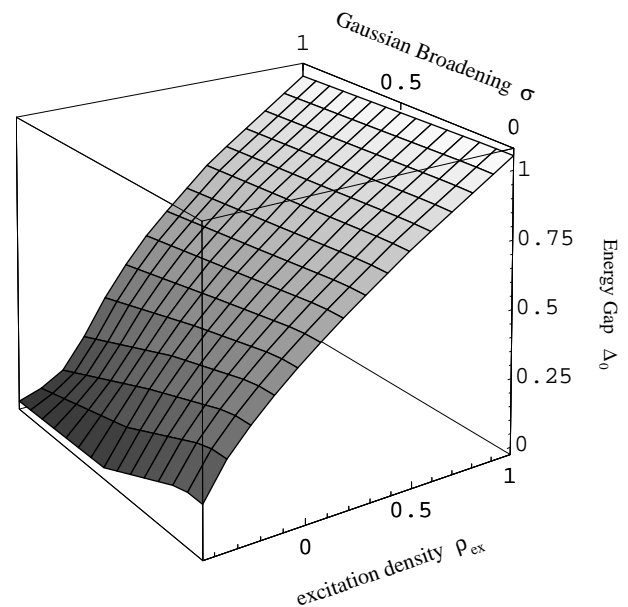


FIG. 8. Energy gap  $\Delta_0$  in the units of  $g$  in the absence of decoherence as a function of excitation density  $\rho_{ex}$ , and Gaussian broadening,  $\sigma$ .

In the degenerate case the magnitude of the gap in the density of states is given by (33). If we consider an inhomogeneous broadening of excitonic energies with a Gaussian distribution then there will always be some oscillators with energies which make the term  $(\epsilon - \mu/2)^2$  vanish and thus, strictly, the magnitude of the gap would be  $2g\langle\psi\rangle - 4\gamma_1$  at all excitation densities. This means that the gap would vanish at  $\langle\psi\rangle \rightarrow 0$  in contrast to degenerate case in which its magnitude would be  $g - 4\gamma_1$ . However, the contribution of these states, arising only from the tails of the Gaussian distribution, would be very small essentially leading to a soft gap of the magnitude of  $g - 4\gamma_1$  at very low densities as in degenerate case.

We call  $\Delta_0$  the gap in the absence of decoherence when  $\gamma_1 = 0$ . Omitting the case when  $n_{exc} = 0$ , discussed above, we calculate numerically the magnitude of the gap, in the units of the dipole coupling  $g$ , for a wide

range of excitation densities and inhomogeneous broadening  $\sigma > 0$ .  $\Delta_0$  very much depends on the excitation density. The Gaussian broadening of energies decreases the gap at low densities but has almost no influence at high excitation densities. In the presence of the decoherence (homogeneous broadening) the actual gap  $\Delta$  would be

$$\Delta = \Delta_0 - 4\gamma_1 \quad (34)$$

Fig. 8 and equation (34) can be used to estimate the magnitude of the gap in particular experimental systems in which the values of broadenings, density and the dipole coupling is known. Some estimates of the magnitude of the energy gap in particular materials and conditions were reported in a brief report [17].

### VIII. APPLICABILITY OF THE MODEL AND THE METHOD

As already stated in Section II, the model of two-level systems interacting only via cavity photon field gives a reliable description of tightly bound, Frenkel-type excitons localised by disorder or bound on impurities, molecular excitons in organic materials, atoms in the solid state or Josephson junctions arrays in microwave microcavities. In the classical limit  $\lim_{N \rightarrow \infty} (\langle n_{ex} \rangle / N) = \rho \rightarrow const.$  it has an exact solution of the mean-field form

$$|\lambda, u, v\rangle = e^{\lambda\psi^\dagger} \prod_j (v_j b_j^\dagger + u_j a_j^\dagger) |0\rangle. \quad (35)$$

However, the case of Wannier excitons propagating in the sample, present in some clean semiconductors (for example GaAs quantum wells), is conceptually not very different. The sums over sites in the microscopic Hamiltonian would have to be replaced with sums over momentum states and Coulomb interactions between electrons and holes would have to be included. Such a model without photons was studied by Keldysh and Kopayev [14] and for coherently driven semiconductor by Schmitt-Rink et al. [18]. If we treat the Coulomb interaction on the mean-field level then the natural extension of the Keldysh mean-field wave-function to account for photons will be

$$|\Psi_0 \rangle = e^{\lambda\psi_0^\dagger} \prod_{\vec{k}} [u_{\vec{k}} + v_{\vec{k}} b_{\vec{k}}^\dagger a_{\vec{k}}] |0\rangle, \quad (36)$$

which is of analogous form to that for the two-level systems case (35). Then the influence of the various decoherence processes can be included in exactly the same way as described in Section II.

At the level of mean-field, we do not expect that the change of the model from that of two-level oscillators to free electron and holes with a Coulomb interaction would cause any dramatic differences. It was shown within the mean-field techniques of Keldysh [14,15,19] that the Coulomb interaction has a pairing effect and leads to a

formation of a coherent excitonic insulator phase and this would only be enhanced by the dipole coupling.

At high excitation densities (large photon fields) the dipole interaction between excitons and photons is the dominant interaction. In the case of a driven excitonic system Schmitt-Rink *et al* [18] pointed out that for a very large pumping, and thus high excitation densities, the Coulomb interaction is just a very minor correction to the dominant dipole coupling. They also state that, in the absence of the Coulomb interaction, their results for propagating electrons and holes are equivalent to those obtained for an ensemble of independent two-level oscillators as optical transitions with different  $\mathbf{k}$  decouple.

The Coulomb interaction would be more important at low densities. However, in this case, the dominant contribution arising from the interaction between an electron and hole within the same exciton, is taken into account in model studied in this work. All other Coulomb interactions are much weaker and, as with the dipole coupling, favour condensation.

Although we do not expect qualitative differences, it would be interesting, especially at low excitation densities, to perform similar calculations in the momentum representation with the Coulomb interaction. This would allow one to study the relative influence of the two independent pairing mechanisms, namely the dipole coupling and Coulomb interactions, on the condensate.

Summarising, our method of including and studying the decoherence effects is general and can be applied in the same way as in this work to propagating excitons as well as to coherently driven condensates. The coherent photon field in the driven system is an external, fixed, parameter and not a self-consistent field satisfying equation (20). In contrast the gap in the density of states, proportional to the coherent field amplitude, is present exactly as for an equilibrium condensate. The model can be applied to obtain a qualitative description of the physical behaviour even for propagating or weakly bound excitons. It would give similar predictions to the model based on propagating electrons and holes with Coulomb interactions treated within the mean-field approximation. It does not, however, include screening and other non mean-fields effects.

If the microscopic origins of the decoherence processes are known for a particular experimentally studied system, the theory could be extended to include this information. The detailed account of the coupling constants and the density of states for the environment can be easily included within this framework. In this work we have assumed a static bath or Markovian (Ohmic) bath but in general the bath propagators are frequency dependent and thus  $\langle \psi \rangle$  would depend on frequency as in the Eliashberg theory of gapless superconductors [20,21]. The phenomenological constants  $\gamma_1$  and  $\gamma_2$  can thus be, in principle, obtained from this microscopic calculation for a particular system.

The results presented in this work are performed at zero temperature for which the summations over the

Matsubara frequencies in (20), (21) and (23) become integrals and are performed numerically. The extension to finite temperatures is straightforward. At finite temperatures the summations over a discrete  $\nu_n$  can be performed using the standard techniques [22] and thus finite temperatures could be easily studied.

A much more important extension than the finite temperature case is the problem of non-equilibrium systems. For a system with very strong pumping and decay processes the thermal distribution of the relevant quasiparticles cannot be assumed. The influence of non-equilibrium distributions on the polariton condensate will be published elsewhere.

### IX. REMARKS ON EXPERIMENTAL REALISATION OF BEC OF POLARITONS

While stimulated scattering into the lower polariton branch (reminiscent of Bose statistics) was clearly observed and reported by several groups [23–32], there is still no evidence of excitonic coherence, and therefore BEC of polaritons. The experiments that have been performed fall into two categories. In the first, polaritons are pumped coherently, with a laser having an angle of incidence chosen at a “magic angle” close to the bottom of the lower polariton branch. In the second set of experiments the pumping is incoherent. The laser pumping is tuned to be well above the ground state so that polaritons have to undergo several inelastic scattering events before reaching the ground state and thus losing the initial coherence of the pump.

Although not yet measured, the potential coherence of polaritons in the experiments of the first category would be inherited from the pump and the behaviour could be explained in terms of parametric oscillation. Experiments of the second category could be potential candidates for spontaneous BEC of polaritons but evidence for it are very sparse. The coherence of the photon field emitted at polariton frequency has recently been measured in one experiment [28] but this alone does not prove that there is a coherence in the excitonic part. A laser is an example where coherent photon field is generated without large excitonic coherence. A more direct evidence of excitonic coherence is necessary. Large excitonic coherence would map to a large gap in the excitation spectrum which should be seen in the incoherent luminescence.

Experiments on cavity polaritons which report the stimulated scattering into the lower polariton branch are performed at low densities to avoid the fermionic phase space filling effect, so that two clear polariton peaks could be seen. For such densities the gap in the excitation spectrum would be very small and easily suppressed by the decoherence processes in the sample. Indeed such a gap has never been observed in the photoluminescence spectrum. The attempt to increase the density of polaritons in these experiments results not in the formation of

the condensate but in a switching into the weak-coupling regime and lasing.

This is not surprising since the increase in the density of polaritons in these experiments is obtained by increasing the pumping of excitons. Incoherent pumping is a pair-breaking decoherence process and thus the increase in the pumping intensity results in the increase of not only the density of excitons but also decoherent scattering. As shown by Eastham and Littlewood [9], the fermionic structure of excitons does not prevent condensation, even at very high densities. Thus, in the current experiments, we suggest that it is not a phase-space filling effect which lead to a laser as the pump intensity is increased, but the increase in the decoherence strength. If the polariton condensate is ever to be observed an increase in density without an increase in decoherence is necessary.

Localised and tightly bound excitons, such as excitons in disordered quantum wells or Frenkel-type excitons in organic compounds, seem to be better candidates for observing a polariton condensate than the high-quality GaAs quantum wells with weakly bound, delocalised excitons. Static disorder is not a pair-breaking effect and would have a weaker influence on the condensate than screening and ionisation in the case of delocalised or weakly bound excitons. Additionally the polariton splitting reported in organic materials is as large as 80 meV [5,6] in comparison to the upper bound of 20 meV in GaAs. Another very good candidate for observation of effects described in this work would be atoms in solid state, glass spheres, dilute atomic gases in which the dephasing is particularly weak in comparison to the dipole coupling.

### X. SUMMARY

We have studied the equilibrium Bose condensation of cavity polaritons in the presence of decoherence. It has been shown [12] that the widely used Langevin equations with the constant, frequency independent decay rates are not valid for systems with large polarisation in which the gap in the density of states is present. In the regime of weak decoherence these processes have to be treated self-consistently, in such a way that the gap in the density of states is taken into account. We have proposed a self-consistent method analogous to the Abrikosov and Gor’kov theory of gapless superconductivity [1] which allow us to study all regimes of the system as the decoherence is changed from zero to large values and for a wide range of excitation densities.

We have found that at small decoherence the polariton condensate is protected by the energy gap in the excitation spectrum. The gap is proportional to the coherent field amplitude and thus the excitation density, so the condensate, unlike the excitonic insulator [19], is more robust at high densities. This gap gets smaller and

eventually is completely suppressed as the decoherence is increased. We have shown that there is a regime, analogous to the gapless superconductor, when the coherent fields are present without an energy gap. This regime, at very high excitation densities, has most of the features of a photon laser.

We have studied the influence of two different types of processes, both pair-breaking and non-pair-breaking ones as well as inhomogeneous broadening of the energy levels. We have shown that only the pair-breaking processes can lead to phase transitions. Non-pair-breaking processes and inhomogeneous broadening of energies can quantitatively change the behaviour of the system but cannot prevent condensation.

We have studied a general form of the interactions, introducing pair-breaking and non-pair-breaking processes and thus our theory is applicable to a wide range of systems. For more detailed results, the particular origin of the interactions and thus the particular density of states for the baths have to be taken into account.

We have studied the whole phase diagram of the system given by the Hamiltonian (4) for different values of the decoherence strength, inhomogeneous broadening and the excitation densities and established the crossover between an isolated polariton condensate and a photon laser as the decoherence strength is increased.

Our results suggest that, in contrast to traditional lasers, coherent light can be generated without a population inversion. This work generalised the existing laser theories to include the gap in the excitation spectrum caused by the coherence in a media in the low decoherence regime.

## XI. ACKNOWLEDGEMENT

We would like to thanks F. M. Marchetti and P. R. Eastham for helpful discussions concerning mathematical techniques. MHS acknowledge the support of research fellowship from Gonville and Caius College, Cambridge.

- 
- [1] A. A. Abrikosov, L. P. Gor'kov, *JETP* **12**, 1243 (1960)
- [2] M. G. Raizen, R. J. Thompson, R. J. Brecha, H. J. Kimble, and H. J. Carmichael, *Phys. Rev. Lett.* **63**, 240 (1989).
- [3] C. Weisbuch, M. Nishioka, A. Ishikawa, and Y. Arakawa, *Phys. Rev. Lett.* **69**, 3314 (1992).
- [4] A. Tedicucci, Y. Chen, V. Pellegrini, M. Borger, L. Sorba, F. Beltram, and F. Bassani, *Phys. Rev. Lett.* **75**, 3906 (1995).
- [5] D. G. Lidzey, D. D. C. Bradley, M. S. Skolnick, T. Virgili, S. Walker, and D. M. Whittaker, *Nature* **395**, 53 (1998).
- [6] D. G. Lidzey, D. D. C. Bradley, T. Virgili, A. Armitage, M. S. Skolnick, and S. Walker, *Phys. Rev. Lett.* **82**, 3316 (1999).
- [7] R. Rapaport, R. Harel, E. Cohen, A. Ron, and E. Linder, *Phys. Rev. Lett.* **84**, 1607 (2000).
- [8] P. Barbara, A. B. Cawthorne, S. V. Shitov, and C. J. Lobb, *Phys. Rev. Lett.* **82**, 1963 (1999).
- [9] P. R. Eastham, P. B. Littlewood, *Solid State Commun.* **116**, 357 (2000), *Phys. Rev. B* **64**, 235101 (2001).
- [10] For the quantum theory of the laser developed by Haken, Risken, Lax, Louisell, Scully and Lamb see M. O. Scully and M. S. Zubairy, *Quantum Optics* (Cambridge University Press, Cambridge, U.K., 1997).
- [11] H. Haken, *Rev. Mod. Phys.* **47**, 67 (1975); *Laser Theory*, Springer-Verlag 1984.
- [12] M. H. Szymanska, P. B. Littlewood, unpublished. In (6) the life-time for a single two-level oscillator is generalised to many two-level systems without taking into account any collective effects. It can be shown that if we couple every two-level system to its own distinct bath we recover Equation (6). Such a method and so (6) is unphysical if the interactions between two-level system generated for example by the photon field is substantial. The environment needs to be coupled to the whole ensemble of two-level oscillators and averaged out in the selfconsistent way.
- [13] K. Hannewald, S. Glutsch and F. Bechstedt, *J. Phys. Condens. Matter* **13**, 275 (2001)
- [14] L. V. Keldysh and Y. V. Kopaev, *Fiz. Tverd. Tela* **6**, 2791 (1964), [*Sov. Phys. Solid State* **6**, 2219, (1965)].
- [15] L. V. Keldysh and A. N. Kozlov, *Zh. Eksp. Teor. Fiz.* **54**, 978 (1968), [*Sov. Phys. JETP* **27**, 521 (1968)].
- [16] J. Zittartz, *Phys. Rev.* **164**, 575 (1967)
- [17] M. H. Szymanska, P. B. Littlewood, *Solid State Commun.* **124**, 103 (2002)
- [18] S. Schmitt-Rink, D. S. Chemla, and H. Haug, *Phys. Rev. B* **37**, 941 (1988).
- [19] C. Comte and P. Nozières, *J. Phys. (Paris)* **43**, 1069 (1982).
- [20] G. M. Eliashberg, *Zh. Eksperim. i Teor. Fiz.* **38**, 966 (1960), [*Sov. Phys. JETP* **11**, 696 (1960)].
- [21] D. J. Scalapino, in *Superconductivity*, edited by R. D. Parks, volume 1, chapter 10, pages 449–560, Marcel Dekker, Inc., New York, 1969.
- [22] G. Rickayzen, *Green's Functions and Condensed Matter* (Academic Press Inc., London, 1987).
- [23] L. S. Dang, D. Heger, R. André, F. Bœuf, and R. Romestain, *Phys. Rev. Lett.* **81**, 3920 (1998).
- [24] P. Senellart and J. Bloch, *Phys. Rev. Lett.* **82**, 1233 (1999).
- [25] F. Boef, R. Andre, R. Romestain, L. S. Dang, *Phys. Rev. B* **62**, R2279 (2000).
- [26] A. Alexandrou, G. Bianchi, E. Peronne, B. Halle, F. Boeuf, R. Andre, R. Romestain, L. S. Dang, *Phys. Rev. B* **64**, 233318 (2001).
- [27] V. Pellegrini, R. Colombelli, L. Sorba, and F. Beltram, *Phys. Rev. B* **59**, 10059 (1999).
- [28] H. Deng, G. Weihs, C. Santori, J. Bloch, Y. Yamamoto, *Science* **298**, 199 (2002).
- [29] J. J. Baumberg, P. G. Savvidis, R. M. Stevenson, A. I.



- Tartakovskii, M. S. Skolnick, D. M. Whittaker, and J. S. Roberts, *Phys. Rev. B* **62**, R16247 (2000).
- [30] P. G. Savvidis, J. J. Baumberg, R. M. Stevenson, M. S. Skolnick, D. M. Whittaker, and J. S. Roberts, *Phys. Rev. Lett.* **84**, 1547 (2000).
- [31] R. M. Stevenson, V. N. Astratov, M. S. Skolnick, D. M. Whittaker, E. Emam-Ismael, A. I. Tartakovskii, P. G. Savvidis, J. J. Baumberg, and J. S. Roberts, *Phys. Rev. Lett.* **85**, 3680 (2000).
- [32] M. Saba, C. Ciuti, J. Bloch, V. Thierry-Mieg, R. Andre, Le Si Dang, S. Kundermann, A. Mura, G. Bongiovanni, J. L. Staehli, B. Deveaud, *Nature* **414**, 731 (2001)
- [33] C. Liu, Z. Dutton, C. H. Behroozi, L. V. Hau, *Nature* **409**, 490 (2001)